RAPID COMMUNICATIONS

PHYSICAL REVIEW E VOLUME 51, NUMBER 1 JANUARY 1995

Tilted arrays of dendrites

Raz Kupferman
School of Physics and Astronomy, Raymond and Beverly Sackler Faculty of Exact Sciences, Tel Aviv University, Tel Aviv 69978, Israel

David A. Kessler
Department of Physics, Bar-Ilan University, Ramat Gan 52900 Israel
(Received 19 September 1994)

We report on the existence of tilted arrays of dendrites in solidification. It arises from a long-wavelength instability of the infinite array. The connection to the parity-broken dendrites recently discovered is pointed out. We show that the array is stable to short distance fluctuations explaining the existence of a stable envelope for solidification patterns.

PACS number(s): 68.70.+w, 61.50.Cj, 64.60.−i, 64.70.Dv

The problem of dendritic growth is one of the classical problems of pattern formation [1–4]. The major breakthrough in this field occurred a decade ago with the solution for the problem of the isolated dendrite. It was understood that the microscopic dynamics (surface tension, anisotropy) were singular perturbations which give rise to the solvability conditions determining the velocity and shape of the dendrite [5]. While the theory of the isolated dendrite is elegant and amenable to an essentially complete analysis, in practice (both experimentally and in simulations), the isolated dendrite is not the generic morphology encountered. It is not uncommon, for example, to find arrays of dendrites. The theory for such arrays has been the subject of much investigation over the years [6,7], nevertheless it continues to yield surprises. The most recent such surprise was the discovery of the parity-broken dendrite by Brener *et al.* [8]. An array of mirror-image couples of parity-broken dendrites bifurcates [9] from the arrays of symmetric dendrites. In this paper, we demonstrate a new bifurcation to a tilted array as a result of an instability of the array to an antisymmetric mode with Bloch wave number $k=0$.

In this paper we will present the new tilted state, and demonstrate how it arises from the above mentioned instability. The intimate connection of this state to the parity-broken dendrite will then be elucidated. We will also relate these states to their analogs in directional solidification. Finally, we will examine the implications of our stability analysis of the dendritic array for general issues in the morphology of solidification patterns.

A hint that tilted arrays are possible was provided by the numerical simulations of the phase-field model of Kupferman *et al.* [10] (Fig. 1). They observed the spontaneous formation of such arrays by the following mechanism. Four symmetric fingers grow in the direction of maximum surface tension. At the 45° directions, the interface is unstable and undergoes a periodic sequence of tip-splitting, emitting asymmetric fingers which, driven by anisotropy, grow steadily parallel to the main trunks. As these fingers are emitted at constant intervals of time, they build up into a tilted array of dendrites.

In order to investigate both tilted and untilted arrays of dendrites, we consider the standard (one-sided) free boundary model describing crystal growth from a supersaturated solution. Steady-state solutions at velocity v, $\zeta(x)$, satisfy the stationary equation

$$\Delta = 2p\int_{-\infty}^{\infty} dx'\, G[x,\zeta(x);x',\zeta(x')] - \int_{-\infty}^{\infty} ds\, d_0(s)\kappa(s)\frac{\partial G}{\partial n'}[x,\zeta(x);x(s),\zeta(s)], \quad (1)$$

where

$$G(x,y;x',y') = \frac{1}{2\pi} e^{-p(y-y')} K_0[p\sqrt{(x-x')^2+(y-y')^2}]. \quad (2)$$

Length is measured in units of half a unit cell, a, $p=av/2D$ is the dimensionless velocity, and D is the diffusion constant. For an infinite tilted array of identical fingers

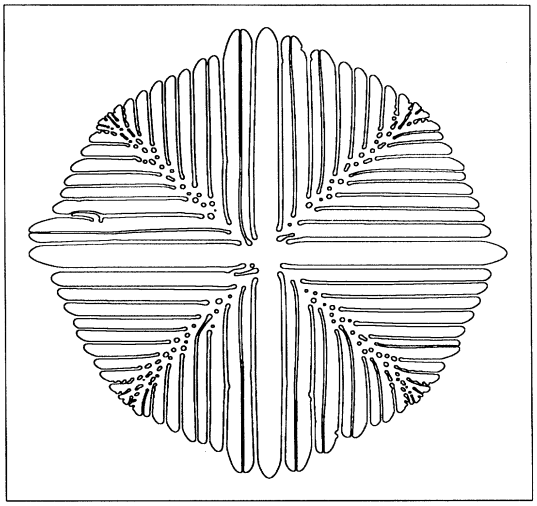

FIG. 1. A late-stage growth pattern obtained for a numerical simulation of the phase-field model for large undercooling ($\Delta=0.8$) and strong anisotropy, reprinted from Ref. [10].

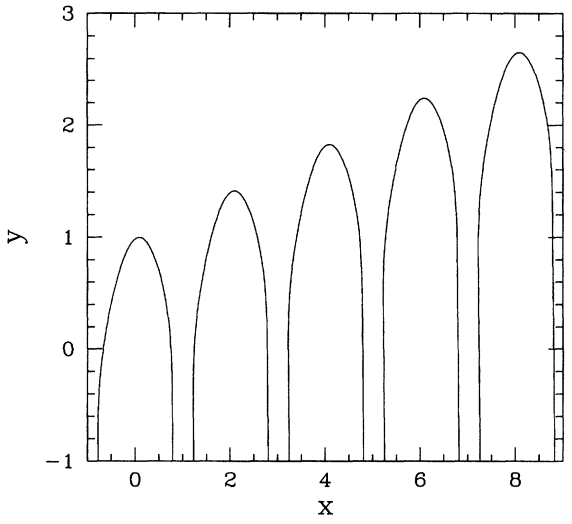

FIG. 2. Solution of a tilted array of dendrites for $\Delta=0.79$, $d_0=0.01$, and $\epsilon=0.1$. The dimensionless velocity is $p=4.25$, and the tilt angle is $\Omega=11.7°$.

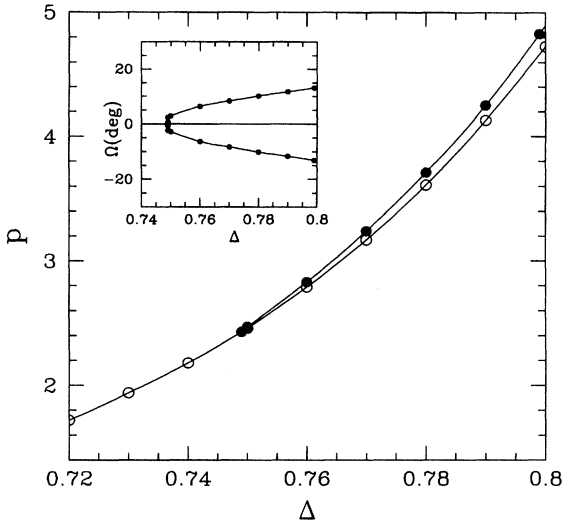

FIG. 3. Velocity versus supersaturation for untilted (open dots) and tilted (solid dots) arrays of dendrites. The inserted plot gives the tilt angle as function of supersaturation.

with tilt angle Ω, it is sufficient to solve $\zeta(x)$ inside a unit cell, $x \in (-1,1)$, applying the translational relation

$$\zeta(x+2n)=\zeta(x)+2n\tan\Omega, \quad n=0,\pm1,\pm2,\ldots . \tag{3}$$

The numerical procedure is then similar to the one employed to find parity-broken dendrites (see Ref. [9] for details). If $\zeta(x)$ is discretized into N points, it forms together with p and Ω a total of $N+2$ unknowns. These are determined by Eq. (1) evaluated at the $N-2$ interior points, supplemented by boundary conditions for ζ and ζ' on both ends. This set of nonlinear algebraic equations is then solved by Newton's method.

In Fig. 2 we show a tilted array of dendrites obtained using the above procedure. The velocity as function of supersaturation is plotted in Fig. 3 for $d_0=0.01$ and $\epsilon=0.1$ (we consider here only the fastest branches of solutions which correspond to the most stable ones). Solutions of untilted arrays are identical to those of a single symmetric dendrite in a channel. A branch of untilted arrays exists here for $\Delta\gtrsim0.62$. At $\Delta\simeq0.75$ a branch of tilted arrays bifurcates off the branch of the untilted ones. The tilted dendrites are faster by a few percent. The difference in the velocities is relatively small as p is large ($\gtrsim2.5$); hence the diffusion field near the tip of the dendrite is almost unaffected by the relative position of the neighboring dendrites.

The appearance of tilted arrays is related to a parity-breaking instability of the untilted array. To calculate the stability spectrum of an array of dendrites, we adapt the method which was employed for arrays of Saffman-Taylor fingers [11], and for cellular patterns in directional solidification [12]. The basic steps are to consider the time-dependent evolution equation of the interface, and substitute a solution of the form

$$\zeta(x,t)=\zeta(x)+\delta(x)e^{\omega t}, \tag{4}$$

where $\zeta(x)$ is the stationary solution, and $\delta(x)$ is a small perturbation. We use the standard quasistatic approximation. As $\zeta(x+2n)=\zeta(x)$, the linearized operator acting on $\delta(x)$ is also periodic, and therefore it is possible to construct Bloch eigenstates of the form

$$\delta(x)=e^{i\frac{k}{2}x}\psi_k(x), \tag{5}$$

where $k \in (0,\pi)$ is the wave number of the modulation, and $\psi(x+2n)=\psi(x)$. It is then possible to separate the stability equation into its real and imaginary parts, obtaining two coupled eigenvalue equations for ω. Repeating this procedure for all k, a band structure of the stability spectrum, $\omega(k)$, is obtained.

In Fig. 4 we plot the two least stable eigenvalues, ω, as a function of the Bloch wave number for $\Delta=0.75$ (i.e., just above the bifurcation point). The symmetric mode necessarily vanishes for $k=0$, due to the translational invariance in y. For small values of k, ω is positive, but becomes increasingly negative for larger k. The antisymmetric mode has a positive eigenvalue for $k=0$. The zero mode due to the translation symmetry in x has been eliminated by our choice of parametrization of the perturbation, (4), since $\delta(x)$ for such a mode is unbounded. An unstable antisymmetric mode of infinite wavelength is precisely the tilt instability we looked for. Table I shows that the appearance of the branch of tilted arrays coincides with the onset of the unstable mode. Also for the antisymmetric mode, ω becomes negative for larger k.

Another noteworthy point is that antisymmetric modes for $k=\pi$ are identical to the antisymmetric modes for a single finger in the channel geometry. The eigenvalues of the highest antisymmetric mode as function of Δ are given in Table I for $k=0$ and $k=\pi$. As described above, the onset of the tilt instability occurs slightly below $\Delta=0.75$. For larger Δ, $\omega(k=0)$ increases as the entire band becomes less stable,

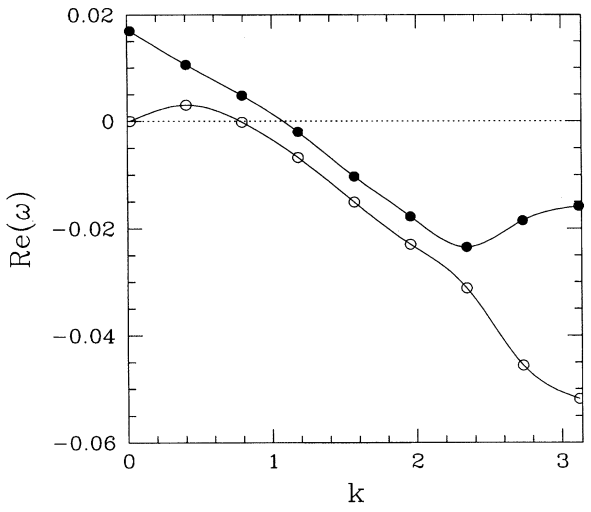

FIG. 4. Eigenvalues of the least stable modes as function of the Bloch wave number for $\Delta=0.75$. The open (solid) dots represent the least stable symmetric (antisymmetric) mode.

until for $\Delta=0.76$ it becomes entirely unstable. At this point, where $\omega(k=\pi)=0$, a second bifurcation is expected to occur—the appearance of mirror-image couples of parity-broken dendrites. We checked, and indeed found such solutions to emerge at that point. Thus the instabilities responsible for the appearance of these two apparently different types of parity-broken patterns are nothing but the two extreme points of the same band of the stability spectrum of an array of symmetric dendrites.

The bifurcation to the tilted pattern is, of course, one of the basic instabilities for cellular patterns characterized by Coullet and Iooss [13]. As such, it is directly analogous to the bifurcation to traveling waves in directional solidification [12]. Similarly, parity-broken states exist in both systems. However, whereas in directional solidification these bifurcations can be traced back to the interaction of the q-$2q$ unstable modes of the planar interface, no such connection can be made in our case where the cells are intrinsically of infinite amplitude. For this reason, the existence of these new patterns in solidification eluded investigators for a very long time.

The stability diagram presented in Fig. 4 merits further discussion. The relative stability of the large k modes, compared to the $k=0$ mode, is contrary to the known behavior for arrays of Saffman-Taylor fingers [11]. In that system, the high-k modes were increasingly unstable, reflecting the presence of a renormalized Mullins-Sekerka instability at long length scales. In the present case, there appears to exist a

TABLE I. Eigenvalues of the least stable antisymmetric mode for $k=0$ and $k=\pi$.

Δ	$\omega\ (k=0)$	$\omega\ (k=\pi)$
0.65	−0.001	−0.09
0.67	−0.005	−0.03
0.69	−0.009	−0.06
0.71	−0.010	−0.10
0.73	−0.003	−0.06
0.75	**+0.017**	−0.02
0.77	**+0.064**	**+0.05**
0.79	**+0.165**	**+0.16**

restoring force for short-wavelength modulation of the array's front. Such a restoring force acts like an effective surface tension, tending to preserve a smooth front (envelope). The existence of a stable envelope for sufficiently high undercooling has been previously demonstrated in the context of mean-field theories for algorithmic growth models [14]. It has been suggested that a stable envelope is an intrinsic feature of solidification at finite undercooling. The relevant length scale for this restabilization has not yet been analyzed, but is presumably related to the diffusion length. This would explain the absence of such restabilization in the case of Saffman-Taylor fingers. Furthermore, the stability of the envelope appears to be correlated to the internal branching structure of the pattern [15]. Our calculation provides a rigorous evidence of an envelope stabilizing mechanism, and hopefully will shed light on the physical origins of this phenomenon, and its impact on the large scale dynamics of the solidification process.

To conclude, we demonstrated that the range of steady-state solutions for solidification patterns is much richer than has been previously believed. It is plausible that the scope of solutions is even wider, in particular when considering the arrangement of multiple growth elements into a global morphology. Completely open yet is the question of what determines the dynamically selected patterns when there exists more than one stable solution.

We are grateful to E. Ben-Jacob, O. Shochet, H. Levine, and L. Kramer for many valuable discussions. Figure 1 is part of a joint work with E. Ben-Jacob and O. Shochet. This study was partially supported by a grant from the G.I.F., the German-Israeli Foundation for Scientific Research and Development, and by Grant No. 9200051 from the United States—Israel Binational Science Foundation (BSF). D.A.K. is supported by the Raschi Foundation. He also acknowledges the partial support of the U.S. DOE Grant No. DE-FG-02-85ER54189.

[1] D. A. Kessler, J. Koplik, and H. Levine, Adv. Phys. **37**, 255 (1988).

[2] J. S. Langer, Science **243**, 1150 (1989).

[3] E. Ben-Jacob, and P. Garik, Nature **343**, 523 (1990).

[4] E. A. Brener and V. I. Mel'nikov, Adv. Phys. **40**, 53 (1991).

[5] These steady-state solutions are more properly needle crystals. Dendrites arise from sidebranching perturbations of the steady-state solutions. We shall adopt common practice and not distinguish between needle crystals and dendrites in the rest of the paper.

[6] D. A. Kessler, J. Koplik, and H. Levine, Phys. Rev. A **34**, 4980 (1986).

[7] E. Brener, M. Geilikman, and D. Temkin, Zh. Eksp. Teor. Fiz. **94**, 241 (1988) [Sov. Phys. JETP **67**, 1002 (1988)].

[8] E. Brener, H. Müller-Krumbhaar, Y. Saito, and D. E. Temkin, Phys. Rev. E **47**, 1151 (1993).

[9] R. Kupferman, D. A. Kessler, and E. Ben-Jacob, Physica A (to be published).

[10] R. Kupferman, O. Shochet, and E. Ben-Jacob, Phys. Rev. E **50**, 1005 (1994).

[11] D. A. Kessler and H. Levine, Phys. Rev. A **33**, 3625 (1986).

[12] H. Levine and W-J. Rappel, Phys. Rev. A **42**, 7475 (1990); H. Levine, W-J. Rappel, and H. Riecke, *ibid.* **43**, 1122 (1991); W-J. Rappel and H. Riecke, *ibid.* **45**, 846 (1992); W-J. Rappel, Phys. Rev. E **48**, 4118 (1993).

[13] P. Coullet and G. Iooss, Phys. Rev. Lett. **64**, 866 (1990).

[14] Y. Tu, H. Levine, and D. Ridgeway, Phys. Rev. Lett. **71**, 3838 (1993).

[15] O. Shochet, K. Kassner, E. Ben-Jacob, S. G. Lipson, and H. Müller-Krumbhaar, Physica A **181**, 136 (1992); **197**, 87 (1992).